Knowledge-based Engineering and Sciences (2024), **5**, (2), 54–74
doi:10.51526/kbes.2024.5.2.54-74

RESEARCH PAPER

Assessment of Landscape Change and its Relationships with Surface Temperature and Geo-spatial Indices during 1992 - 2022 at Haldia Industrial Region, West Bengal, India

Shyam Pada Karan,*[,1] Swati Mandal,[2] and Suman Das[3]

[1]Research Scholar, Department of Geography, Panskura Banamali College (Autonomous), Purba Medinipur, West Bengal, India
[2]Associate Professor, Department of Geography, Panskura Banamali College (Autonomous), Purba Medinipur, West Bengal, India
[3]Research Scholar, Department of Remote Sensing and GIS, Vidyasagar University, Midnapore-721102, West Bengal, India
*Corresponding author. Email: shyampadakaran@gmail.com

(Received 30 April 2024; revised 13 August 2024; accepted 25 August 2024; first published online 31 August 2024)

Abstract

Unplanned local development and alterations in Land Use and Land Cover (LULC) are an early alert for towns and cities around the world. The population pressure has resulted in the conversion of natural land into impermeable areas, which has altered the surface energy budget and created microclimatic differences locally. The main objective of the present study is to estimate LULC changes and its relation to increases Land Surface Temperature (LST) in the Haldia Industrial Region (HIR) of West Bengal using multi-temporal Landsat 5 Thematic Mapper (TM) of 1992 and Landsat 8 Operational Land Imager (OLI) of 2022 with 30-m spatial resolution images were obtained from the USGS website. The supervised classification method was applied by using Maximum Likelihood classification (MLC) to classify the satellite images into various LULC classes such as settlement, waterbody, vegetation, agriculture land, and fallow land, respectively. The result suggested an overall increase of settlement area from 13.49 km^2 in 1992 to 44.54 km^2 in 2022. On the other hand, the agriculture land decreased from 214.26 km^2 to 152.34 km^2 due to fast urbanization, decline green lands, and expansion of barren lands. The outcome result from LST was exhibited that the LST value has increased 3.77°C during 1992 to 2022 in this study area. The Normalized Difference Vegetation Index (NDVI) was showed a strong negative relationship with LST with a determination coefficient (R^2) values found as 0.491 (1992) and 0.356 (2022). The positive determination coefficient between LST with Normalized Difference Water Index (NDWI) was found as 0.0002 (1992), and 0.0417 (2022). R^2 values were estimated as 0.174 (1992), and 0.0347 (2022) between LST with Normalized Difference Built-up Index (NDBI) that indicated a positive determination coefficient. The findings enhanced understanding of the relationship between urban LST and LULC in developing an inclusive climate resilience policy and making the HIR more sustainable to the effects of climate change.

Keywords: Land use and land cover; Landsat images; Land surface temperature; Climate change; Haldia Industrial Region.

1. Introduction

One of the essential components of sustainable development and global environmental change is land use and land cover change (LULCC) [1], [2]. LULCC is primarily caused by anthropogenic activity [3]. Increased agricultural and industrial activity as a result of rapidly expanding population has resulted in significant changes in LULC and increased demands on natural resources stored in the land [4]. Urbanization, climate change, and economic expansion are three current environmental issues that affect LULC and have a significant impact on the environment's ecosystem [5]. Therefore, in order to plan for the future and manage natural resources, it is crucial to recognise these changes, evaluate their patterns, and consider how they affect the environment. LULCC is growing mostly because to human activity [6], [7].

Researchers, planners, and decision-makers use LULC data to assess urban growth trends and track changes in natural resource availability [1], [8]. The biodiversity, water and radiation budgets, trace gas emissions, and other processes that interact to affect the climate and biosphere are also impacted by these changes in LULC [9]. LULCC identification, however, continues to be the most straightforward evidence of human influence on the land [10]. Given this, it is crucial to measure LULCC and determine its implications in order to create effective targeted policy solutions. In order to close the gap between science and policy, this study aims to produce innovations and other products that promote more environmentally friendly land management methods.

Rapid LULC change has significant effects on both human and natural settings [11]. One of these effects is the rise in Land Surface Temperature (LST) [12]. The physical processes responsible for the land surface balance of water, energy, and CO2 are greatly influenced by the LST, an estimate of the real ground temperature [13]. LST has been used to gather data on a variety of land uses and land covers because of its sensitivity to different land superficial features [14]. Urban regions typically experience elevated temperatures known as Urban Heat Islands (UHI) due to increased solar radiation absorption, thermal capacity, and conductivity [11].

Another important environmental and socio-economic concern caused by LULC modification is desertification, which occurs at all sizes (global, regional, and local) [15]. Many studies have used the Normalised Difference Vegetation Index (NDVI) to extract vegetation abundance from remotely sensed data, and it has also been used to estimate the amount of desertification by quantifying vegetation cover features [16]. The NDVI compensates for changing lighting conditions, surface slope, and viewing angle and is thus particularly effective for monitoring vegetation at the continental to global scale. Satellite remote sensing has proven to be a valuable data source for mapping and monitoring the spatial distribution of LST [17] and NDVI, satellite remote sensing has established itself as a crucial data source [18].

To remedy this shortcoming, the integration of Remote Sensing (RS) and Geographic Information System (GIS) data will offer tremendous potential for unearthing, portraying, monitoring, and assessing LULCC and forest change [19]. The current study will use geospatial data to establish the spatiotemporal pattern of LULC changes in the Haldia Industrial Region (HIR), allowing decision makers to grasp the dynamics of our changing environment and ensure sustainable development. As a result, the goals of this study are to quantify the spatiotemporal changes in Land Use and Land Cover in HIR between 1992 and 2022, to evaluate changes in NDVI and LST of the study area and to assess the effect of LULCC on LST and NDVI.

This study is unique in that it proposes a system for updating LULC information over the study area. Assessment and mapping of LULC change is crucial for sustainable development and environmental change. On the other hand, this study is also emphasized the thermal condition over this region during 1992–2022 time period. The geospatial based analysis is highlighted the status of vegetation, waterbody, and built up area. The findings from this study can help and guide the planners and decision-makers to make a sustainable development of areas with similar backgrounds.

2. Literature Review

The current trend of increases in LULC in various parts of the world is impacted by both anthropogenic activities and biophysical variables [20], [21], [22], [23]. Rapid population expansion, excess housing demand, and socioeconomic development all contribute to an increase in urbanised area [24], [25]. On the other hand, industrialisation, deforestation, reduction in agricultural land, urban expansion, and population growth are the primary reasons for changing the LULC [24], [26], [27], [28], [29]. These changes in LULC are also the major driver of changes in LST, with the growth of impervious surfaces having a significant impact. This change is one of the primary factors for increasing the LST around the world [21], [22], [23], [24], [25], [26], [27], [28], [29]. In this sense, GIS and remote sensing are ideal tools for land-cover monitoring, urban/regional analysis, and investigating spatiotemporal changes in LULC on a local to global scale. Thus, satellite pictures such as Landsat are extensively utilised for environmental monitoring, particularly to assess the impact of LULC change on LST variability. Overall, this study provides useful information regarding changes in LULC patterns and may aid in identifying places that have seen major land use changes, which may have implications for urban planning and management.

3. Study Area

Haldia is one of the fastest growing port base industrial clusters of Purba Medinipur district in the state of West Bengal in Eastern India (Figure 1). The geographical extension between 22°00'44"N to 22°12'26"N latitude and 87°56'00"E to 88°11'37"E longitude. Formally it is situated on the deltaic plain of Ganges. The area is located about 125 km. south west of state capital Kolkata and 50 km. from Bay of Bengal near the mouth of the rivers Hooghly and Haldi in Purba Medinipur district. This region is bounded by distinct physical boundaries namely the Hooghly River (North-North Eastern, Eastern and South-South Eastern side), Haldi River (South-South Western side) and Hijli Tidal Canal (North-Western side) respectively. The total areal coverage in the study region is about 326.85 km^2 out of which 9.20 km^2. area has already submerged in the water within the area. So, actual area of interest (AoI) is 317.65 km^2. (i.e. excluding submerged area). The entire study area comprises on 1 Municipality (Haldia) with 26 wards, 3 Community Development Blocks (2 full- Sutahata and Haldia and 1 part- Mahishadal), 18 Gram Panchayat (14 full and 4 part) and 2 Census Towns (Garhkamalpur and Barda) [30], [31].

HIR is well connected by roadways, railways and waterways in and abroad. The 4-Lane NH 41(Now NH 116) connects Haldia with NH 6 at Kolaghat along with SH 4 connects NH 41 at Mechada. Haldia is connected by rail via Panskura, situated on the Howrah-Kharagpur section of the South-Eastern railway to the rest of the country and the circular rail line connecting also the core industrial area to provide sliding facilities. This area consisted by four major ferry service viz. Haldia Township-Kendyamari, Balughata-Nandigram, Kukrahati-Raichak and Kukrahati-Diamond Harbour and Geonkhali-Nurpur ferry service across the Rivers Hooghly and Haldi. Not only have the roads, rail and ferry but also a helipad or air serviced available there [32]. The land in the HIR is almost flat, the ground level is 7 ft. to 11 ft. above MSL having a general slope towards southeast and the area is covered by alluvium soil. Although, soil of the coastal belt are slightly saline in nature. The climate of the region is Tropical Savana type which under Aw climate as per Koppen classification. Long monsoon, moderate to severe summer, and short spell of cold weather prevail in this region. As per early revenue records of the area express that natural forest become dwindling as far back as 1830. Some stray species of trees, shrubs and herbs are found today [33]. It has different types of industries such as fertilizer plant, petrochemical and downstream industries, automobile industry, food processing industry, logistic hub, sugar refinery, biodiesel industry and edible oil industry, etc. [30] Indian Journal of Spatial Science. Total population of the study region is 548062 with the density of population about 1676.80 persons per km^2. The male population constitute of 51.73 per cent and female is 48.27 percent and the gender ratio is 933 female per 1000 male [31].

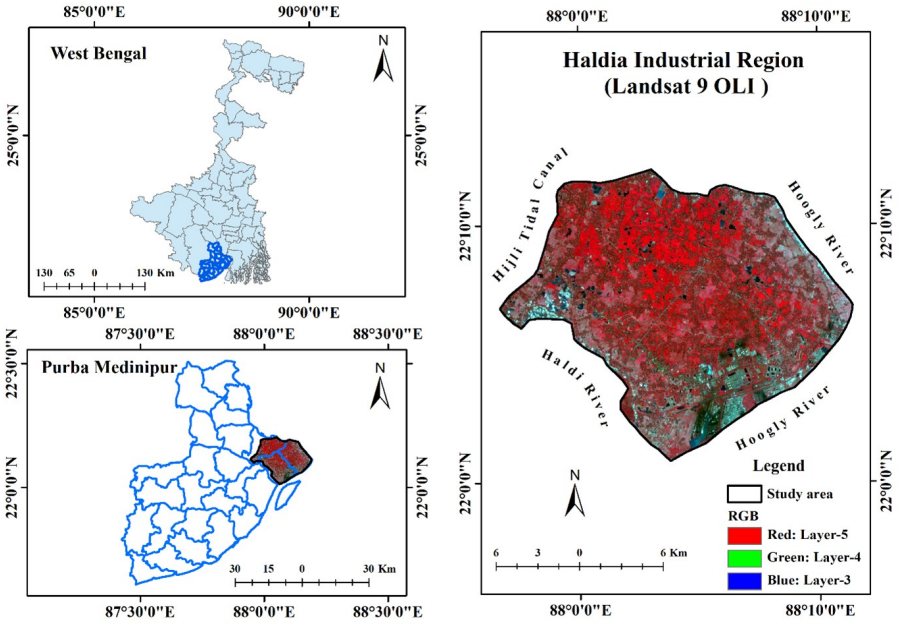

Figure 1: *Study area map of Haldia Industrial Region.*

4. Materials and Methods

4.1 Data use

The present study has utilized Landsat TM (1992) and OLI/TIRS (2022) data for the analysis of LULC change analysis and also the environmental effect using LST and NDVI of the study area. The remotely sensed datasets were acquired from the United States Geological Survey (USGS) earth explorer website [34]. Two thermal bands (band 6 for Landsat TM and band 10 for Landsat OLI/TIRS) were used to identify the LST of the Haldia Industrial Region (HIR). On the hands, Red and Near Infra-Red bands were used to estimate the NDVI. Table 1 illustrates the description of satellite employed in the present study to evaluate the LULC change and environmental effect.

Table 1: *Descriptions of satellite datasets used in the study.*

Date/Year	Sensor	Spatial resolution(m)	Path/Row	Data source
1992-04-09	Landsat 5 TM	30	138/045	https://earthexplorer.usgs.gov/
2022-03-19	Landsat 8 OLI/TIRS	30	138/045	

4.2 Image pre-processed and classification

At first, the satellite images were pre-processed such as geometric, atmospheric, and topographic corrections by the use of remote sensing software. ERDAS Imagine 2014 software was used for layer stacking, masking, and sub-setting the area of interest (AOI) of this study. In this study, the supervised classification technique of Maximum Likelihood Classification (MLC) was adopted to classify the Landsat images. Many researchers are found that MLC has higher accuracy in detecting the LULC classification [27,35–37]. The True Colour Combination (TCC) and Standard False Colour Combination (SFCCs) were visually investigated to select the training samples. Five LULC classes (Table 2) like settlement, vegetation, fallow land, agriculture land and waterbody were classified

using MLC-supervised classification. The detail methodological flowchart is shown in the [38] Figure 2.

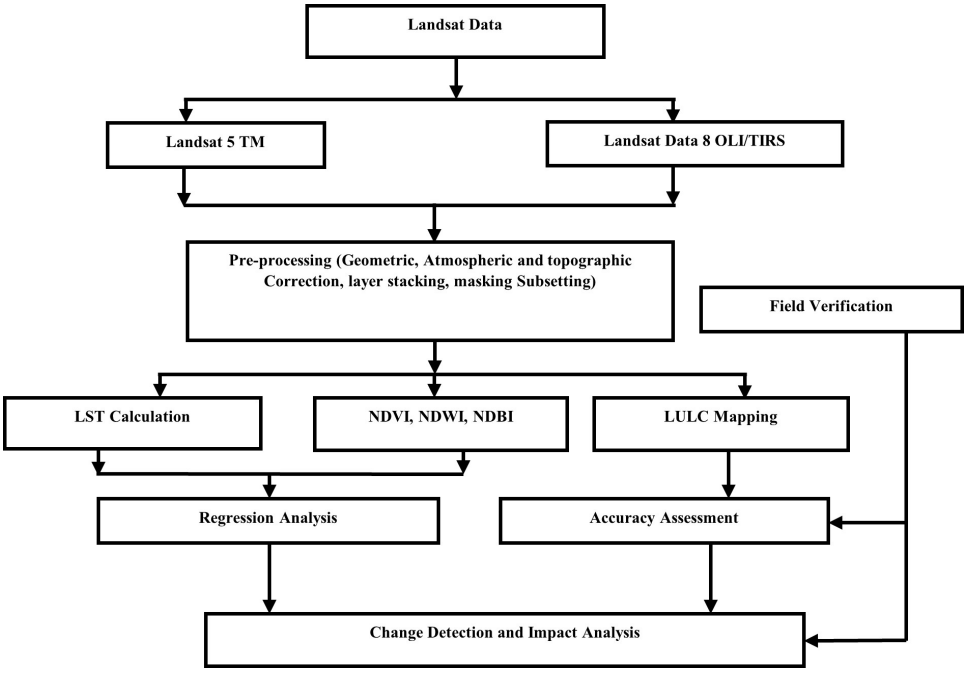

Figure 2: *Detail flowchart of the study.*

Table 2: *Description of the LULC classes [39].*

Sl. No.	LULC classes	Description
1	Settlement	Residential area, Industrial area, transportations, roads and construction area
2	Waterbody	Tidal canal, pond, lake and waterbodies
3	Vegetation	Area having plantation or natural forest including tress, open vegetated area
4	Agriculture Land	Crop land and others seasonal cultivation
5	Fallow Land	Waste area, barren land and also some unseasoned aquaculture area

4.3 Accuracy assessment and kappa statistic

The accuracy assessment was calculated by the Erdas Imagine 2014 software after the classification. After classification, accuracy assessment was the most essential aspect since it shows the accuracy of the classification result [40]. This method was used to compare the data to the ground truth and classify it. Field surveys and Google Earth Pro were used to acquire ground truth data. For classification accuracy, the Non-parametric Kappa test was used. The Kappa coefficient (Table 3) was a diagonal element as well as an element in the confusion matrix [34]. This equation (Eq.(1)) was used to compute the Kappa coefficient.

$$K = \frac{(\text{Observed accuracy} - \text{Chance accuracy})}{(1 - \text{Chance accuracy})} \tag{1}$$

Table 3: *Scale of Kappa coefficient.*

Sl No.	Value of K	Strength of agreement
1	<0.20	Poor
2	0.21 - 0.40	Fair
3	0.41 - 0.60	Moderate
4	0.61 - 0.80	Good
5	0.81 - 1.00	Very good

4.4 Normalized Difference Vegetation Index (NDVI)

Normalized Difference Vegetation Index (NDVI) was used to identify the vegetation cover on the earth surface and observed the area of urban vegetation or not, using remote sensing data [3]. NDVI represents the vegetation scenario of the earth surface which was maintain the local climate variable like precipitation [41]. The NDVI value is located in - 1 to +1; values around 0 are representing the area under poor vegetation such as barren land and built-up land. The values close to the plus one (+1) represent the healthy vegetation and forest cover area all through near minus one (-1) shows water body area of the study location. The NDVI equation is (Eq. (2))

$$NDVI = \frac{(NIR - R)}{(NIR + R)} \tag{2}$$

Where, NDVI = Normalized Difference Vegetation Index; NIR = near infrared band; R = visible red band.

4.5 Normalized Difference Water Index (NDWI)

The NDWI, a remote sensing image-based indicator, is developed by Gao [42] to enhance the water-related features of the landscapes and is used in estimating the leaf content at canopy level. According to Gao, NDWI is a good indicator for vegetation water content and is less sensitive to atmospheric scattering effects than NDVI. This index is derived from the near-infrared and shortwave infrared bands using the following equation:

$$NDWI = \frac{(GREEN - NIR)}{(GREEN + NIR)} \tag{3}$$

The range of NDWI products varies between 1 and +1, depending not only on the leaf water content but also on the vegetation type and cover. High NDWI (in blue) value is related to high vegetation water content and high vegetation cover, while low NDWI values (in yellow) correspond to low vegetation water content and low vegetation fraction cover. NDWI value will decrease during the period of water stress.

4.6 Normalized Difference Built-up Index (NDBI)

NIR, Mid IR (MIR) and Shortwave IR (SWIR) bands were used NDBI in Landsat 5 and 8 images for mapping the built-up and bare land in urban area [43,44]. The values of NDBI range from1 to+1, where 0 to 1 correspond to built-up and value near 1 indicates a high density of built-up area.

$$NDBI = \frac{(SWIR - NIR)}{(SWIR + NIR)} \tag{4}$$

Where, MIR is the middle infrared band (Landsat TM it is band 5 and for Landsat OLI it is band 6) and NIR is the near-infrared band (for Landsat TM it is band 4 and for Landsat OLI it is band 5)

4.7 Land surface temperature calculation

4.7.1 LST for Landsat 5 TM

The LST is prepared using the thermal band of Landsat 5 (band 6) and Landsat 8 (band 10 , band 11). At first, Eq. (3) is calculated for the conversion of digital numbers (DN) values to radiance for Landsat 5 TM . This equation is given below:

1. Conversion of the digital number (DN) to spectral radiance (L) [45] is calculated by (Eq. 5).

$$L_\lambda(\text{LANDSAT5TM}) = L_{min} + \frac{L_{max} - L_{min}}{Qcal_{max} - Qcal_{min}} \times DN \tag{5}$$

Where, L_λ = Spectral Reflectance, L_{min} = Minimum Radiance (1.238), L_{max} = Maximum Radiance (15.303), $Qcal_{min}$ = the minimum DN value of Pixels (1), $Qcal_{max}$ = the maximum DN value of Pixels (255) and DN = Digital number of the pixel value.

2. Conversion of the spectral radiance to temperature in Kelvin [45] is calculated by (Eq. 6).

$$Tb = \frac{k2}{\left(\frac{K1}{L_\lambda} + 1\right)} \tag{6}$$

Where, Tb = the surface temperature (kelvin), K1 = Calibration constant 1 (607.76) and K2 = Calibration constant 2(1260.56)

3. Conversion of Kelvin to Celsius [46] is estimated by (Eq. 7).

$$LST = Tb - 273.15 \tag{7}$$

4.7.2 LST for Landsat 8 OLI

1. Conversion of the digital number (DN) to spectral radiance (L) [27,47,48] is calculated by (Eq. 8).

$$L = \left(\frac{L_{max} - L_{min}}{DN_{max}}\right) \times \text{Band} + L_{min} \tag{8}$$

Where, L = Atmospheric spectral radiance (SR) in watts/ $(m2^*srad^*smp^2)$, Lmax = Maximum spectral radiance (SR) of the DN value, Band Lmin=Minimum spectral radiance (SR) of Band, DNmax = Q cal max –Q cal min = maximum and minimum difference of sensor calibration

2. Using the thermal constants given in the metadata file, the TIRS band data has converted from SR to BT once the DN value are converted to *SR*[47, 48] (Eq. 9).

$$BT = \frac{k2}{\text{Ln}\left(\frac{K1}{\left(\frac{K}{\lambda}\right)} + 1\right)} - 273.15 \tag{9}$$

Where, K 2 and K1 = represents the band specific thermal conversion constants and BT = Brightness temperature in Celsius Calculate of NDVI (Eq. 10).

$$\text{NDVI} = \frac{(\text{NIR} - \text{R})}{(\text{NIR} + \text{R})} \tag{10}$$

3. Proportion of vegetation is calculated by minimum and maximum NDVI value [27,47,48] The Equation is (Eq. 11)

$$PV = Square\left(\frac{NDVI - NDVI_{min}}{NDVI_{max} - NDVI_{min}}\right) \tag{11}$$

4. Land Surface Emissivity (LSE) is calculated based P_v Value. It used the NDVI Thresholds Method- NDVITHM by applying the (Eq.12) [27, 47, 48]

$$\text{LSE} = 0.004 \times P_v + 0.986 \tag{12}$$

5. Conversion of kelvin to Celsius [27, 47, 48] is estimated by (Eq. 13)

$$LST = \frac{BT}{\left\{1 + \left[\frac{\lambda BT}{\rho}\right] \text{In}(LSE)\right.} \tag{13}$$

Where, λ = the wave length of emitted radiance

5. Result and Discussion

5.1 Land use land covers change detection from 1992 to 2022

Water Body, Vegetation, Agriculture Land, Settlement, and Fallow Land are the five LULC classes identified in this study. Rapid urbanization and migration were the primary drivers of urban expansion of the HIR and surroundings. These regional conditions are influenced by business and industrial hubs, as well as transportation and health system accessibility. Following that, anthropogenic activities in this area increased, as did the built-up area. In this study region, approximately 9.79% (4.25% in 1992 and 14.04% in 2022) of settlement area (Table 4) has been increased (Figure 3). In the last 30 years, the city of Haldia has grown rapidly. Both the southern and the south-easterly portions of this study area have undergone significant urbanization [49]. Several researchers have found that the settlement areas were increased day by day due to the population pressure, and also the development of urban areas in different regions over the world [24,27,28]. A total of 31.05 km^2. has been converted to urban land use (Figure 3 - 4). The urban expansion was triggered by port, road, rail, and transportation accessibility, which primarily affected vegetated areas and agricultural land. Around 13.86 km^2 or 4.36% of vegetation area has decreased similarly to 61.92 km^2 or 17.62% of agricultural land also converted into built-up, fallow land (Table 5). Due to human activity, the vegetation was destroyed, and the same thing happened to agricultural land. As the Haldia area developed, the amount of vegetated and agricultural land decreased as the urban area grew toward the middle. More vegetated and agricultural land degradation has been seen in the south. The southern portion of this study area's riverside has seen the majority of the development of urban expansions. Figure 5 - 6 indicate the year-wise LULC classes increased and decreased scenarios. This change in LULC is significant and has an impact on several environmental problems, including heat islands, natural hazards, bio-diversity loss, decreased agricultural land, ecosystem degradation, habitat loss, etc.

Table 4: *Area wise distribution of LULC classes of Haldia Industrial Region.*

LULC classes	1992 (km^2)	% of Area	2022 (km^2)	% of Area
Fallow Land	1.09	0.34	23.24	7.31
Vegetation	92.40	29.13	78.54	24.77
Waterbody	1.96	0.62	18.54	5.84
Settlement	13.49	4.25	44.54	14.04
Agriculture Land	214.26	65.66	152.34	48.04
Total	317.20	100	317.20	100

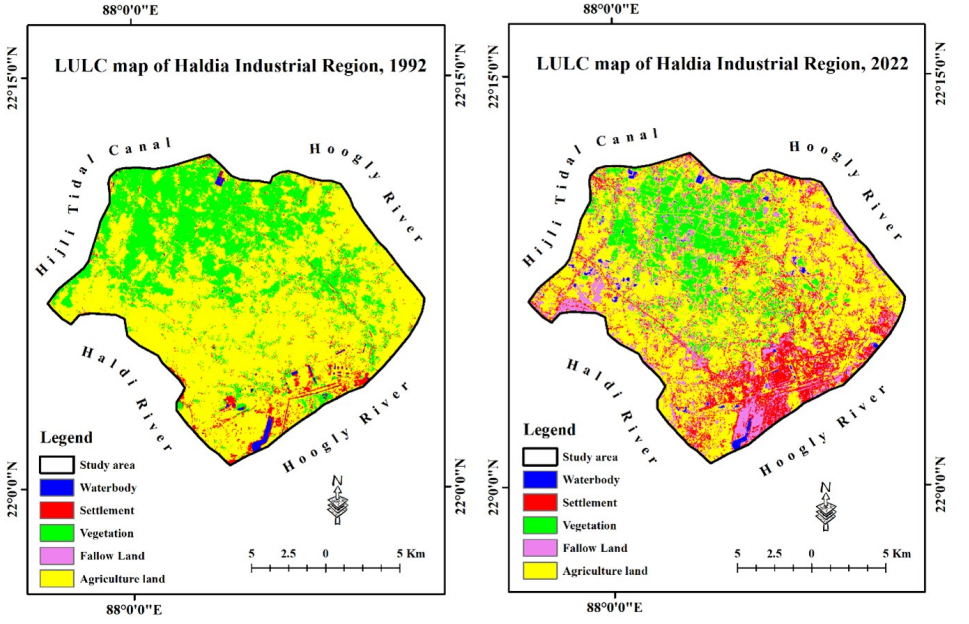

Figure 3: *Land Use Land Cover map (1992-2022).*

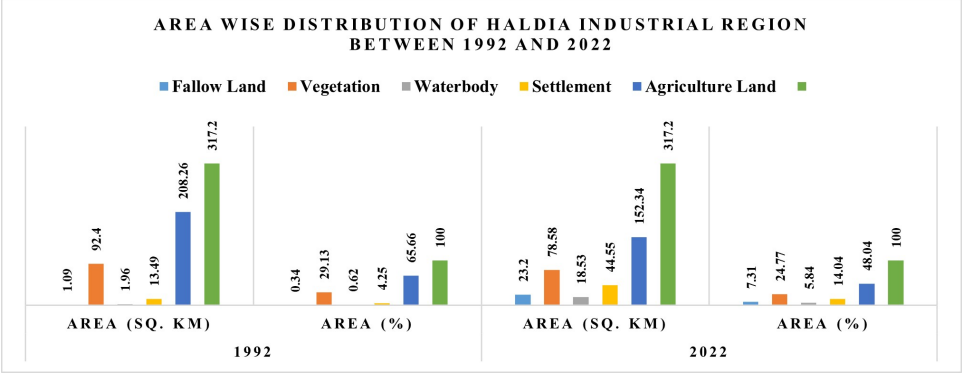

Figure 4: *Area wise distributions of LULC classes (1992-2022).*

5.2 Acuracy Assessment

In this present study, accuracy assessment has been calculated over the LULC classes. The accuracy assessment was conducted over three time periods, utilizing random sample points from all LULC categories. The sample points were selected from each class and, at last, verified with the help of Google Earth images. In 1992, the overall accuracy was 88.24%, which is given in the error matrix calculation table (Table 6). On the other hand, Table 7 was given an overall accuracy of 92.57% for the years 2022. Finally, the accuracy of the classification images has been evaluated using the kappa coefficient, which has very good values of 0.85, 0.91, for the years 1992 and 2022, respectively.

Table 5: *Area wise change of LULC classes over the study area.*

Change of LULC classes (1992-2022)	Area Change (km^2)	Change of LULC classes (1992-2022)	Area Change (km^2)
Settlement - Waterbody	0.077	Waterbody - Agriculture Land	0.119
Settlement - Settlement	3.691	Agriculture Land - Waterbody	0.822
Settlement - Vegetation	0.129	Agriculture Land - Settlement	42.137
Settlement - Fallow land	4.651	Agriculture Land - Vegetation	13.72
Settlement - Agriculture Land	2.849	Agriculture Land - Fallow land	34.2
Fallow Land - Settlement	0.126	Agriculture Land - Agriculture Land	120.82
Fallow Land - Fallow land	0.032	Vegetation - Waterbody	0.767
Fallow Land - Agriculture Land	0.01	Vegetation - Settlement	9.844
Waterbody - Waterbody	1.029	Vegetation - Vegetation	29.454
Waterbody - Settlement	0.247	Vegetation - Fallow land	10.073
Waterbody - Vegetation	0.003	Vegetation - Agriculture Land	41.95
Waterbody - Fallow land	0.515	Grand Total	317.265

Table 6: *Error matrix of LULC in the year of 1992.*

LULC Classes	Reference					Total	CE (%)	UA (%)
	AL	V	W	S	FL			
AL	43	0	0	3	0	46	6.52	93.48
V	0	15	0	0	2	17	11.76	88.24
W	5	0	38	0	0	43	11.63	88.37
S	0	0	0	39	5	44	11.36	88.64
FL	0	0	0	9	45	54	20.00	83.33
Total	48	15	38	51	52	204		
OE (%)	10.42	0.00	0.00	23.53	13.46			
PA (%)	89.58	100.00	100.00	76.47	86.54			
OA (%)	88.24							
KC	0.85							

Table 7: *Error Matrix of LULC in the year of 2022.*

LULC Classes	Reference					Total	CE (%)	UA (%)
	AL	V	W	S	FL			
AL	48	0	0	0	2	50	4.00	96.00
V	0	21	0	0	3	24	12.50	87.50
W	3	0	32	0	0	35	8.57	91.43
S	0	0	0	35	1	36	2.78	97.22
FL	0	0	0	6	51	57	11.76	89.47
Total	51	21	32	41	57	202		
OE (%)	5.88	0.00	0.00	14.63	7.02			
PA (%)	94.12	100.00	100.00	85.37	89.47			
OA (%)	92.57							
KC	0.91							

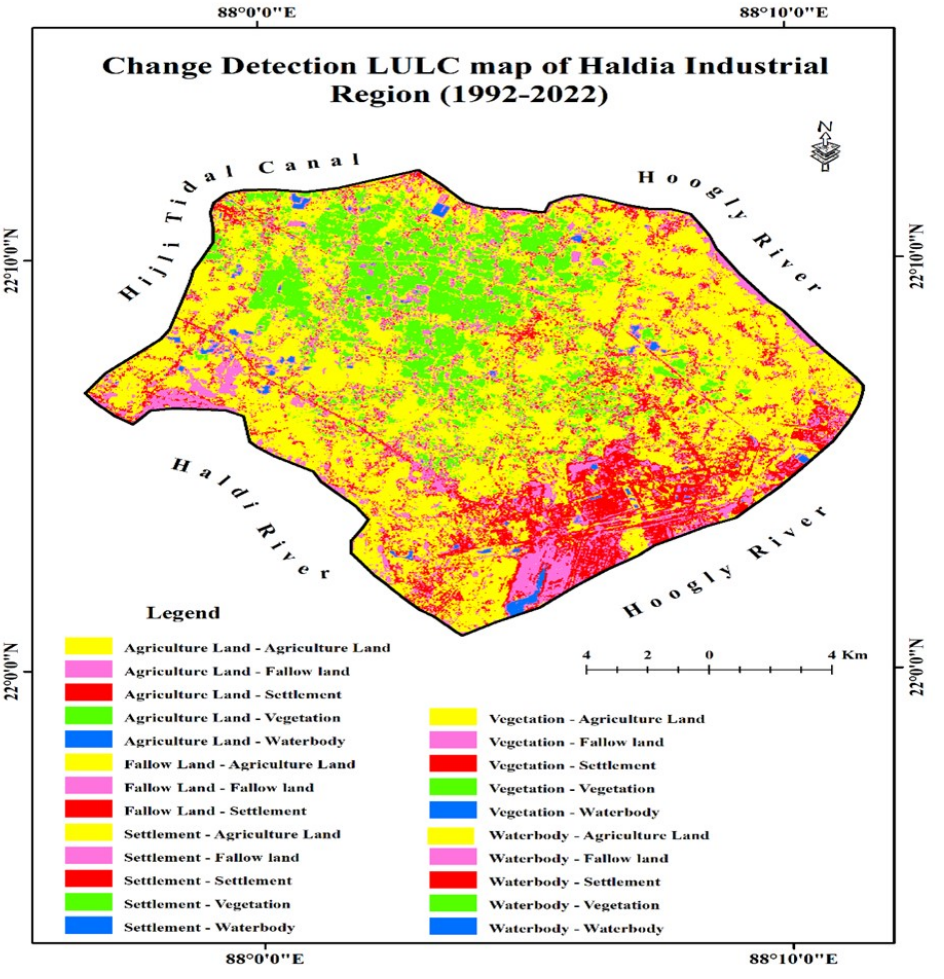

Figure 5: *Change detection map of the study area.*

5.3 Variation of LST

Urban growth caused a significant amount of temperature variation throughout this area. The southern, north, and south-eastern portions of the central region, including Haldia and surrounding areas, experienced high-temperature variation as a result of human activity (Figure 7) shows that the earth's surface temperature variation and highlights the spatial distribution of this study area between the years 1992 and 2022. The temperature content of water is usually lower than other kinds of land uses [21,50]. Any area of this study location experiences the conversion of vegetated and agricultural lands into built-up land. Temperature affects the presence of vegetation. The notified equation was used to derive the spatial and temporal distributions of LST for the years 1992 and 2022 from remote sensing data from the Landsat 5 TM and 8 OLI thermal bands. This map's red colour represented the area's highest temperature, while its yellowish color represented the areas lowest. The LST varies in the year 1992, 25.40°C to 38.77°C with a mean temperature of 32.08°C, and in the year 2022 is 23.46°C to 42.54°C with a mean temperature of 33.00°C (Table 8). The temperature was increased by 3.77°C between the year 1992 to 2022 in HIR and surrounding areas.

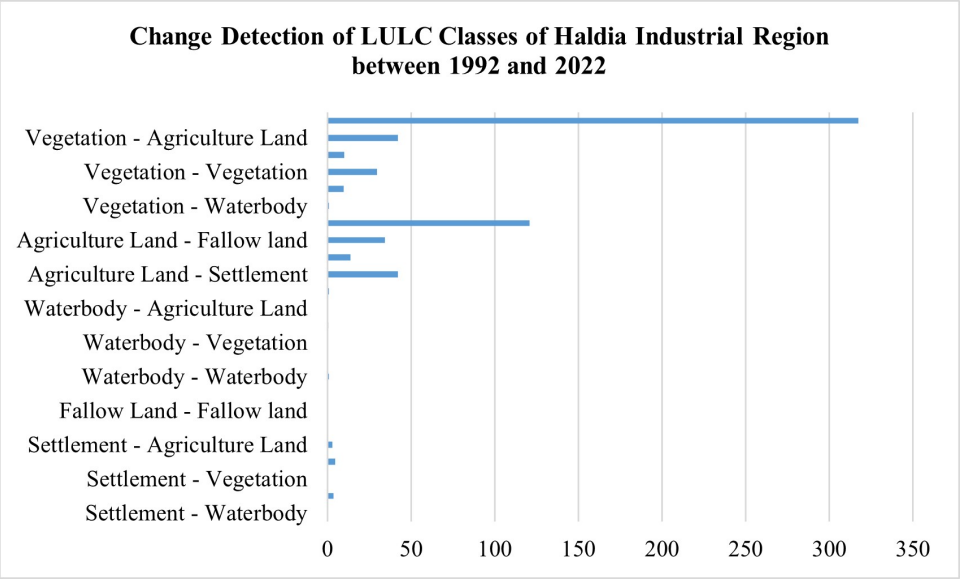

Figure 6: *Conversion of LULC classes of the Haldia Industrial Region.*

Table 8: *Temperature variation on different years of this study.*

Data Used	Min. temperature (°C)	Max. temperature (°C)	Average temperature (°C)
1992	25.40	38.77	32.08
2022	23.46	42.54	33.00

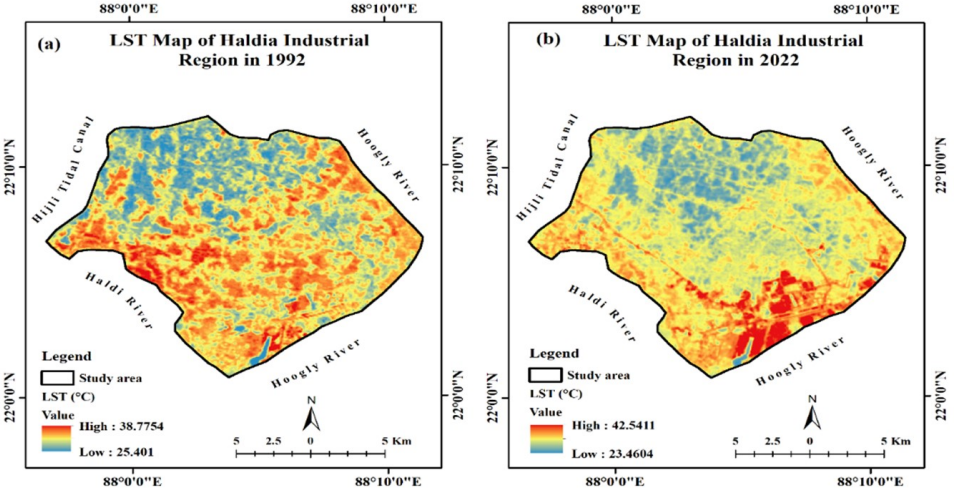

Figure 7: *Land Surface Temperature (LST) map (1992-2022).*

5.4 Estimation of NDVI in 1992 and 2022

Natural vegetation provides a cooling effect on the surroundings [51]. This clearly influences the micro-climate of any urban area. For HIR and in its vicinity, vegetation cover is continuously

decreasing due to increasing population pressure, resulting in urban expansion and land use transformation. These vegetative areas are either completely removed or converted into non-vegetative areas or their density has decreased. In 1992, north-western, and western part of the region had high NDVI values (Figure 8). In 1992, it was 0.55, which has reduced to 0.51 in 2022. These areas had a high density of vegetation, but due to urban expansion, other activities began to emerge, and non-vegetative areas rapidly increased, driving vegetative areas to decline, by 2022, the entire western and north-eastern portions had been turned into impermeable surfaces. Only the northern and middle part of the region has sparse vegetation. Hence, the result of this is clearly seen on the land surface temperature of the area [50].

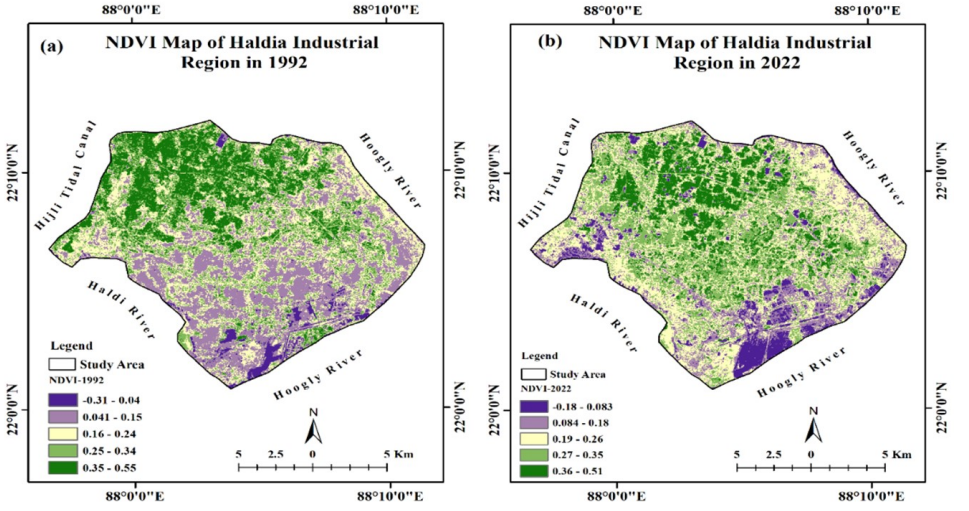

Figure 8: *Normalized Difference Vegetation Index (NDVI) map (1992-2022).*

5.5 Estimation of NDWI in 1992 and 2022

NDWI shows the water content of leaves and is considered a better indicator than NDVI. This index for the research region indicates that the greatest value, which should be less than one, is continuously decreasing. In 1992, it was 0.47, which has reduced to 0.11 in 2022. In this study, it was visible that the water area was increased due to environmental impacts such as floods and also the increase of aquaculture area. This trend indicates that vegetation cover is declining as built-up areas expand. The areas of high value are also reducing, which is very clearly seen in the maps of 1992 and 2022 (Figure 9). Hoque [49] asserts that a body of water can, to some extent, lower both its own and the surrounding temperature.

5.6 Estimation of NDBI in 1992 and 2022

Figure 10a shows the NDBI values for HIR in 1992 and 2022. The figure shows that the minimum value of Landsat 5 image was0.78 in 1992. These values recorded along the all over the study area of the study are due to there was built up and barren land. Actually, the reflectance of settlement and barren land area is same in some of the case. The positive NDBI values demonstrated in the other parts of HIR.

In 2022, the NDBI values for Baghdad ranged between0.29 and 0.48, as shown in Figure 10b. The LULC maps showed a spread of the suburbs of this study area, a large number of informal settlements, especially in agricultural and barren areas. These settlements were concentrated in

southern and towards eastern part Haldia on the river side. Besides, informal settlements spread was noticed in the western and south western of HIR.

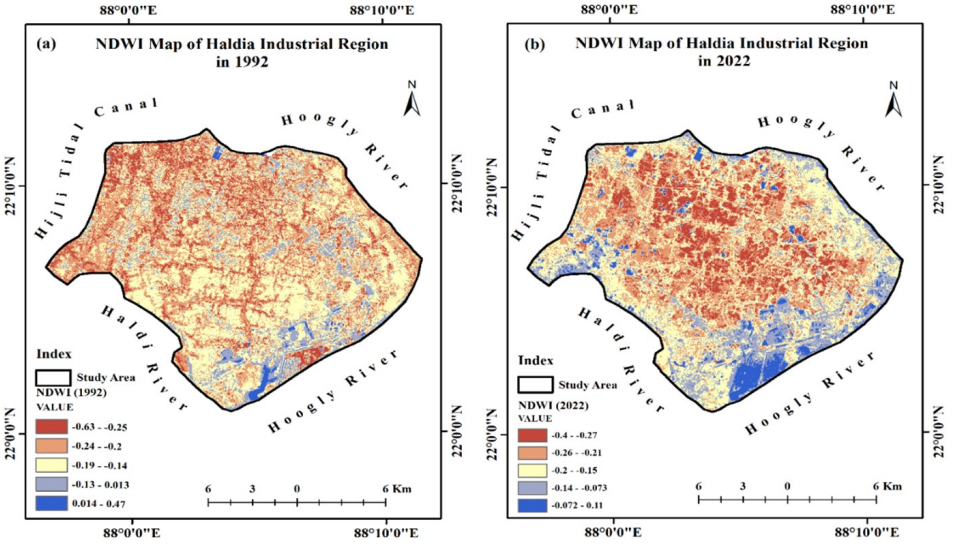

Figure 9: *Normalized Difference Water Index (NDWI) map (1992-2022).*

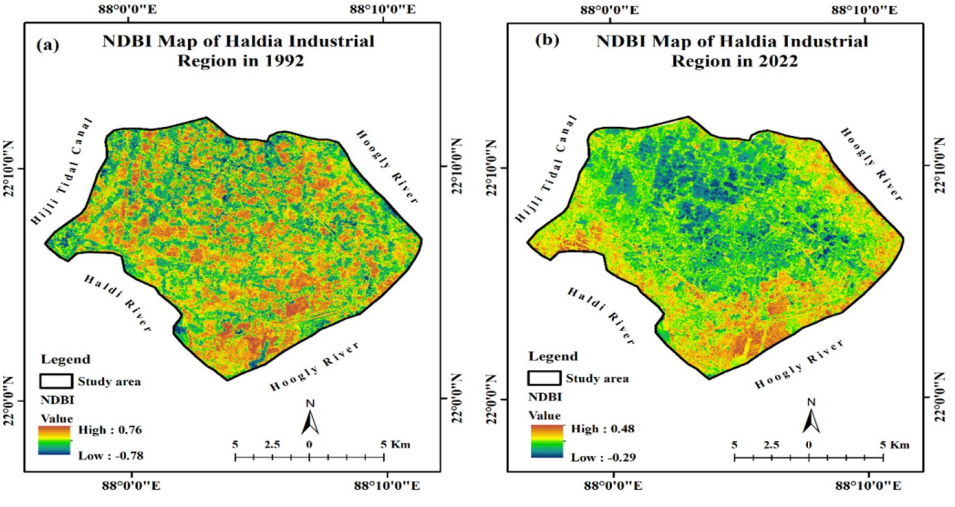

Figure 10: *NDBI map (1992-2022).*

5.7 Correlation of LST and NDVI, NDWI, NDBI

The relationship between LST and LULC map was resulted that the vegetated area showing the low temperature rather than build-up and agricultural land. Thermal variation was different for different LULC classes. The built-up area was hotter than the rest, and the water body was cold. The correlation was estimated using ArcGIS software with the help Microsoft excel and calculated the condition on different years of this study area. The study found a negative correlation between

the NDVI and LST, with R^2 values of 0.3563 and 0.491 in 2022 and 1992, respectively (Figure 11 - 12). This can be attributed to construction activities that generate significant temperature variations and disrupt the vegetated land. According to Hussain and Karuppannan [52], a significant negative correlation was established between LST and NDVI, with higher vegetation cover or biomass resulting in lower LST, depending on the land cover type. Therefore, the relationship between LST and NDWI are presented in Figure 13 - 14. The correlation with LST and NDWI was showing a positive relationship and the R^2 values are 0.0002 and 0.0417 in the years 1992 and 2022 respectively.

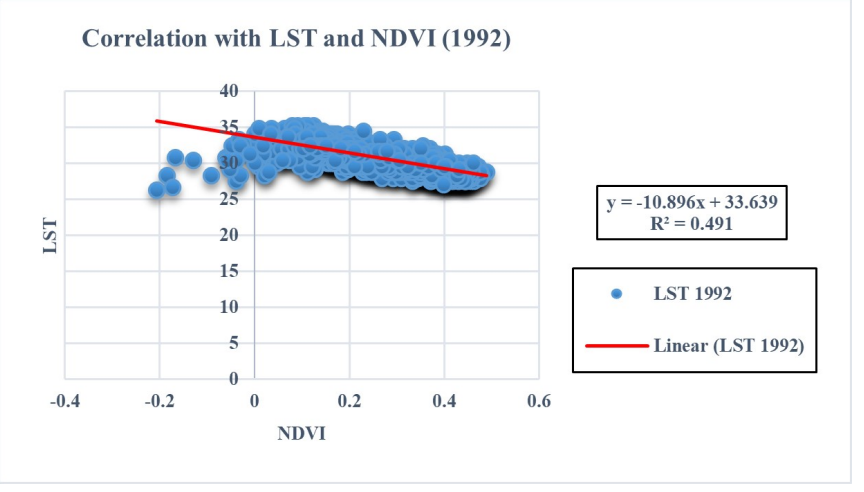

Figure 11: *Correlation with LST and NDVI (1992).*

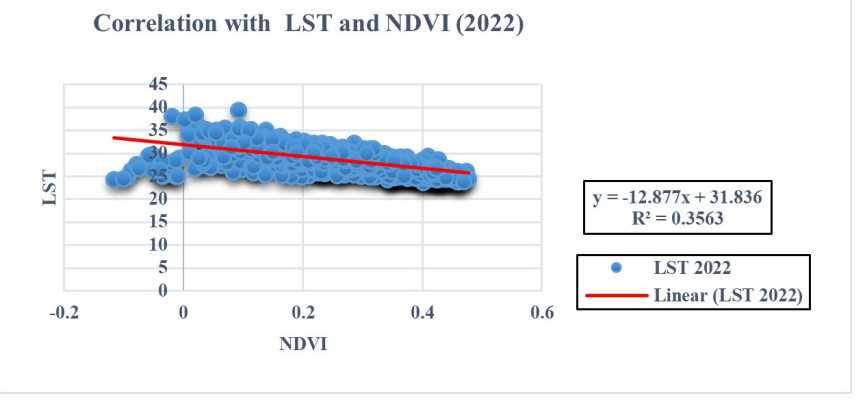

Figure 12: *Correlation with LST and NDVI (2022).*

The correlations between LST and NDBI in 1992 and 2022 are presented in Figure 15 - 16. The results of the linear correlation indicate a positive relationship between LST and NDBI in 1992 and 2022, with R^2=0.1743 and 0.0347, respectively. The built-up and bare areas showed higher LST values in thermal bands of Landsat 5 and 8 compared to other LULC categories, such as vegetation and water. According to Hussain et al., 2023 [53], the findings suggested that the relationship between LST and NDBI was showing a positive correlation with high LST.

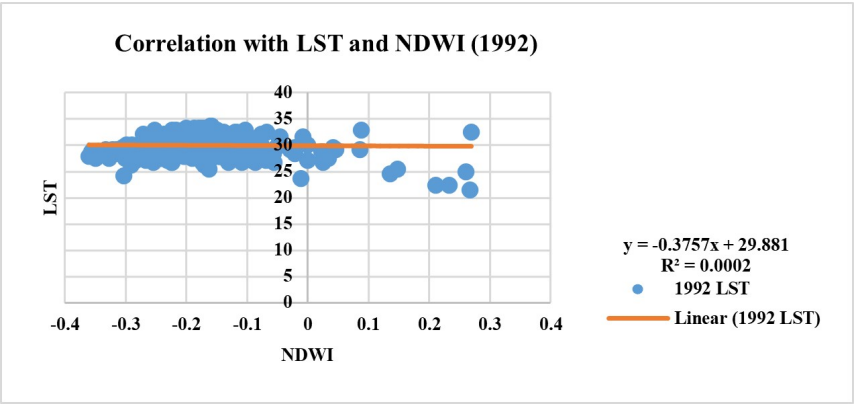

Figure 13: *Correlation with LST and NDWI (1992).*

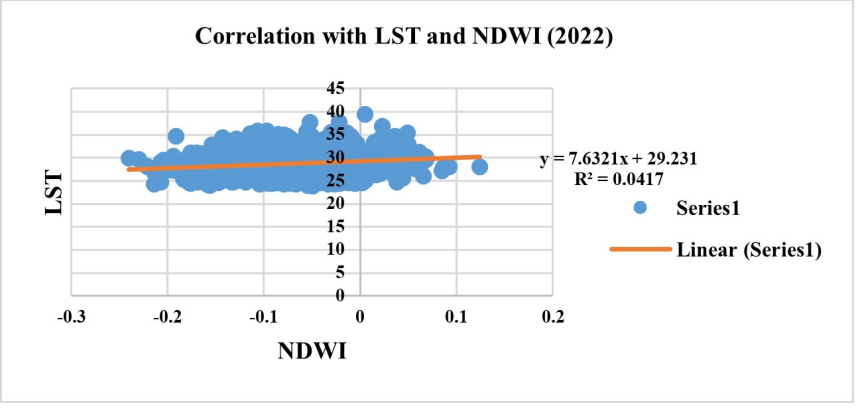

Figure 14: *Correlation with LST and NDWI (2022).*

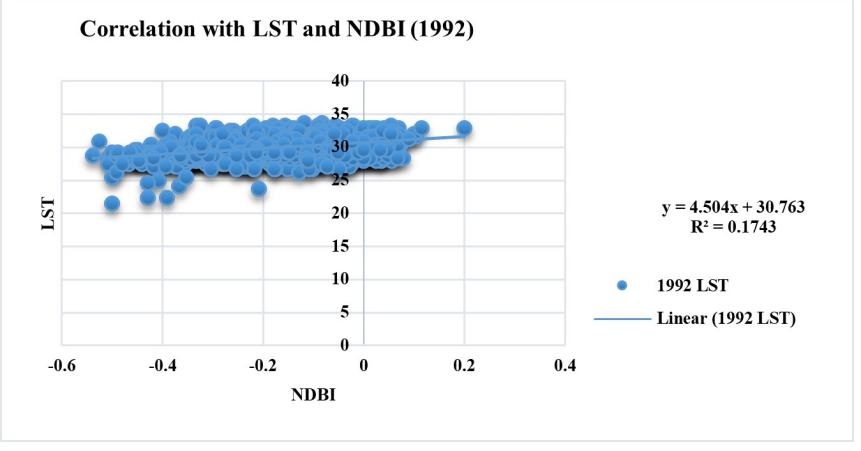

Figure 15: *Correlation with LST and NDBI (1992).*

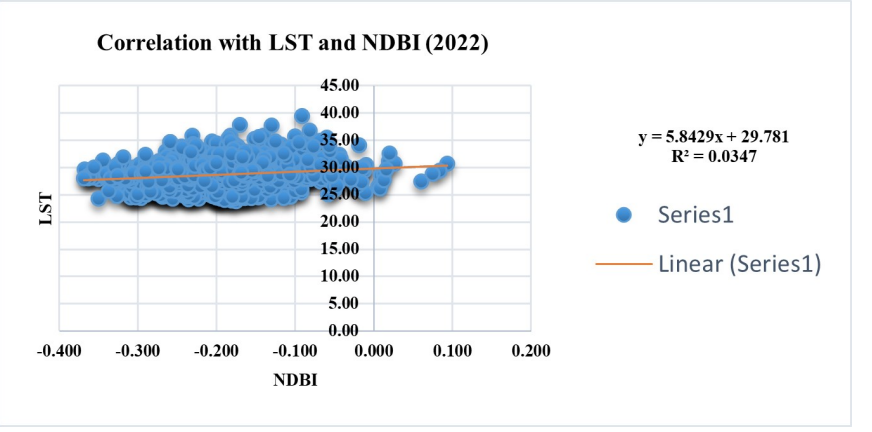

Figure 16: *Correlation with LST and NDBI (2022).*

6. Limitation and future scope

This study demonstrated the mapping LULC, change detection analysis, LST estimation, and correlation between LST and geospatial indices over 30 year's interval (1992–2022). However, this study does not consider seasonal variation of LST over the study area. On the other hand, this research is not estimate the day time and night time surface temperature over this study region. The climatic factors were not accurately analysed during this study. This research only focused on the spatiotemporal correlation between LULC indices with LST. Therefore, in future study, the researcher will calculate the Urban Heat Island (UHI) and Urban Thermal Field Variance Index (UTFVI) for analysing the thermal quality of this study area. This study will be predict future of land dynamics using CA Markov model, ANN model, and also MOLUSCE tool in QGIS software. High resolution such as Sentinel-2A with 10 meter resolution data will be apply for comparative study to monitor the LULC in this study.

7. Conclusion

Multi-temporal Landsat data was collected in this research to detect the LULC alteration and its effect on LST in the HIR area, West Bengal, India. The outcome of LULC classification was highlighted that the settlement area was increased by 4.25% (1992) to 14.04% (2022), while vegetation cover was decreased by 29.13% (1992) to 24.77% (2022) during 1992–2022. On the other hand, fallow land was enlarged by 0.34% (1992) to 7.31% (2022) over the study area. Due to population pressure and accessibility, Haldia has numerous industrial zones and gradually more built-up land. Additionally, the adjacent areas, including Bandar P.H., the Haldia Dock Complex (HDC), Silpaprabesh, Durgachak Town, and Durgachak, have built up their urban areas and improved their transportation connectivity to the mainland cities of Haldia, Howrah, and Kolkata. In a distinct location of this research area, roads and railways connect the urban areas.

Due to anthropogenic activity, urban areas have been the most affected by temperature change in recent decades. The LST values were estimated as 25.40°C to 38.77°C in 1992 and 23.46°C to 42.54°C in 2022 in this study area. Temperature fluctuations in Haldia and the surrounding area have averaged 3.77°C in just thirty years. The Hoogly River serves as the base for the riverine port of Haldia, which is also surrounded by many urban settlements and industrial areas. The urbanization of this study region, however, has a harmful side effect on our environment that offsets this benefit.

LST values were higher in areas with less vegetation cover The NDVI values were shown as 0.55 in 1992, which has declined to 0.51 in 2022. The NDVI trend was reduced from 1992 to 2022

in this study region. Furthermore, this study indicated that NDVI values have a negative correlation with LST. On the other hand, the NDBI showed a positive correlation during this study period. The local ecosystem is being negatively impacted by climate change, which has also led to an increase in human health concerns like respiratory illness, asthma, lung cancer, skin problems, and other diseases. Human respiratory diseases were mostly brought on by air pollution, and this region's water constraint was exacerbated by vegetation deterioration. Even during the rainy season or monsoon around this location, the rate of water infiltration has decreased due to the extensive industrial and construction projects.

For a sustainable water supply and to control the demand for water, rainwater gathering, awareness, planning, and management were required. Areas with vegetation and water bodies showed lower temperatures than the built-up areas. The effects of heat variation and climatic change were primarily felt in urban areas. This area, groundwater pollution, water quality evaluation, land subsidence, urban green space, and evapotranspiration all require further research. This study gives LST and LULC mapping as a foundational resource to aid in the environmental management of Haldia and the adjacent area. These details can be used by the administrative and development authorities to choose a course of action to counteract the effects of changing land surface temperature.

Conflicts of Interest:

The authors declare no conflict of interest.

Abbreviation

AL Agriculture Land
V Vegetation
W Waterbody
S Settlement
FL Fallow Land
CE Commission Error
UA User Accuracy
OE Omission Error
PA Producer's Accuracy
OA Overall Accuracy
KC Kappa coefficient

References

[1] I. E. Olorunfemi, J. T. Fasinmirin, A. A. Olufayo, and A. A. Komolafe, "GIS and remote sensing-based analysis of the impacts of land use/land cover change (LULCC) on the environmental sustainability of Ekiti State, southwestern Nigeria," Environ. Dev. Sustain., vol. 22, no. 2, pp. 661–692, 2018, doi: 10.1007/s10668-018-0214-z.

[2] H. W. Zheng, G. Q. Shen, H. Wang, and J. Hong, "Simulating land use change in urban renewal areas: A case study in Hong Kong," Habitat Int., vol. 46, pp. 23–34, 2015, doi: 10.1016/j.habitatint.2014.10.008.

[3] Q. Weng, "A remote sensing? GIS evaluation of urban expansion and its impact on surface temperature in the Zhujiang Delta, China," Int. J. Remote Sens., vol. 22, no. 10, pp. 1999–2014, 2001.

[4] I. R. Hegazy and M. R. Kaloop, "Monitoring urban growth and land use change detection with GIS and remote sensing techniques in Daqahlia governorate Egypt," Int. J. Sustain. Built Environ., vol. 4, no. 1, pp. 117–124, 2015, doi: 10.1016/j.ijsbe.2015.02.005.

[5] L. Chuanzhe, Y. Fuliang, and L. Jia, "Quantitative study on land use/cover change and driving force in the middle reaches of the Heihe River in the past 20 years," J. Nat. Resour., vol. 26, no. 3, pp. 353–363, 2011.

[6] B. Prenzel, "Remote sensing-based quantification of land-cover and land-use change for planning," Prog. Plann., vol. 61, no. 4, pp. 281–299, 2004, doi: 10.1016/s0305-9006(03)00065-5.

[7] V. N. Mishra, P. K. Rai, R. Prasad, M. Punia, and M.-M. Nistor, "Prediction of spatio-temporal land use/land cover dynamics in rapidly developing Varanasi district of Uttar Pradesh, India, using geospatial approach: a comparison of hybrid models," Appl. Geomatics, vol. 10, no. 3, pp. 257–276, 2018, doi: 10.1007/s12518-018-0223-5.
[8] M. Adeel, "Methodology for identifying urban growth potential using land use and population data: A case study of Islamabad Zone IV," Procedia Environ. Sci., vol. 2, pp. 32–41, 2010, doi: 10.1016/j.proenv.2010.10.006.
[9] J. S. Rawat and M. Kumar, "Monitoring land use/cover change using remote sensing and GIS techniques: A case study of Hawalbagh block, district Almora, Uttarakhand, India," Egypt. J. Remote Sens. Sp. Sci., vol. 18, no. 1, pp. 77–84, 2015, doi: 10.1016/j.ejrs.2015.02.002.
[10] M. F. Iqbal and I. A. Khan, "Spatiotemporal Land Use Land Cover change analysis and erosion risk mapping of Azad Jammu and Kashmir, Pakistan," Egypt. J. Remote Sens. Sp. Sci., vol. 17, no. 2, pp. 209–229, 2014, doi: 10.1016/j.ejrs.2014.09.004.
[11] A. M. Dewan and R. J. Corner, "The impact of land use and land cover changes on land surface temperature in a rapidly urbanizing megacity," 2012 IEEE International Geoscience and Remote Sensing Symposium. IEEE, 2012. doi: 10.1109/igarss.2012.6352709.
[12] S. Pal and O. C. Akoma, "Water Scarcity in Wetland Area within Kandi Block of West Bengal: A Hydro-Ecological Assessment," Ethiop. J. Environ. Stud. Manag., vol. 2, no. 3, 2009, doi: 10.4314/ejesm.v2i3.48260.
[13] C. Kuenzer and S. Dech, Thermal infrared remote sensing: sensors, methods, applications, vol. 17. Springer Science Business Media, 2013.
[14] G. Faqe Ibrahim, "Urban Land Use Land Cover Changes and Their Effect on Land Surface Temperature: Case Study Using Dohuk City in the Kurdistan Region of Iraq," Climate, vol. 5, no. 1, p. 13, 2017, doi: 10.3390/cli5010013.
[15] E.-S. E. Omran, "Detection of land-use and surface temperature change at different resolutions," 2012.
[16] T. Higginbottom and E. Symeonakis, "Assessing Land Degradation and Desertification Using Vegetation Index Data: Current Frameworks and Future Directions," Remote Sens., vol. 6, no. 10, pp. 9552–9575, 2014, doi: 10.3390/rs6109552.
[17] J. A. Voogt and T. R. Oke, "Thermal remote sensing of urban climates," Remote Sens. Environ., vol. 86, no. 3, pp. 370–384, 2003.
[18] B. OS and A. AA, "Change Detection in Land Surface Temperature and Land Use Land Cover over Lagos Metropolis, Nigeria.," J. Remote Sens. amp; GIS, vol. 5, no. 3, 2016, doi: 10.4172/2469-4134.1000171.
[19] E. S. Kasischke et al., Temperate and boreal forests. na, 2004.
[20] F. Ibrahim and G. Rasul, "Urban land use land cover changes and their effect on land surface temperature: Case study using Dohuk City in the Kurdistan Region of Iraq," Climate, vol. 5, no. 1, p. 13, 2017.
[21] S. Pal and S. Ziaul, "Detection of land use and land cover change and land surface temperature in English Bazar urban centre," Egypt. J. Remote Sens. Sp. Sci., vol. 20, no. 1, pp. 125–145, 2017, doi: 10.1016/j.ejrs.2016.11.003.
[22] D. Choudhury, K. Das, and A. Das, "Assessment of land use land cover changes and its impact on variations of land surface temperature in Asansol-Durgapur Development Region," Egypt. J. Remote Sens. Sp. Sci., vol. 22, no. 2, pp. 203–218, 2019, doi: 10.1016/j.ejrs.2018.05.004.
[23] A. Patel, D. Vyas, N. Chaudhari, R. Patel, K. Patel, and D. Mehta, "Novel approach for the LULC change detection using GIS amp; Google Earth Engine through spatiotemporal analysis to evaluate the urbanization growth of Ahmedabad city," Results Eng., vol. 21, p. 101788, 2024, doi: 10.1016/j.rineng.2024.101788.
[24] C. M. Viana, S. Oliveira, S. C. Oliveira, and J. Rocha, "Land Use/Land Cover Change Detection and Urban Sprawl Analysis," Spatial Modeling in GIS and R for Earth and Environmental Sciences. Elsevier, pp. 621–651, 2019. doi: 10.1016/b978-0-12-815226-3.00029-6.
[25] G. Martine, "The sustainable use of space: advancing the population/environment agenda," in cyber seminars of the Population-Environment Research Network, 2001.
[26] S. C. Sam and G. Balasubramanian, "Spatiotemporal detection of land use/land cover changes and land surface temperature using Landsat and MODIS data across the coastal Kanyakumari district, India," Geod. Geodyn., vol. 14, no. 2, pp. 172–181, 2023, doi: 10.1016/j.geog.2022.09.002.
[27] N. Das, P. Mondal, S. Sutradhar, and R. Ghosh, "Assessment of variation of land use/land cover and its impact on land surface temperature of Asansol subdivision," Egypt. J. Remote Sens. Sp. Sci., vol. 24, no. 1, pp. 131–149, 2021, doi: 10.1016/j.ejrs.2020.05.001.

[28] M. Traore, M. S. Lee, A. Rasul, and A. Balew, "Assessment of land use/land cover changes and their impacts on land surface temperature in Bangui (the capital of Central African Republic)," Environ. Challenges, vol. 4, p. 100114, 2021, doi: 10.1016/j.envc.2021.100114.
[29] A.- Al Kafy et al., "Monitoring the effects of vegetation cover losses on land surface temperature dynamics using geospatial approach in Rajshahi City, Bangladesh," Environ. Challenges, vol. 4, p. 100187, 2021, doi: 10.1016/j.envc.2021.100187.
[30] Haldia Development Authority, "Amendment of Land Use and Development Control Plan for Old Haldia Planning Area," 2013.
[31] Census of India, "Government of India (2011). Census of India, District Census Handbook, Medinipur, Director of Census Operations, Kolkata.," 2011. [Online].
Available: https://censusindia.gov.in/census.website/
[32] E. CRIT, Mumbai, "Haldia Region Vision Up-gradation of Perspective Plain (2007). CRIT, Mumbai EMNET Infrastructure, Mumbai, p.21.," 2007. [Online].
Available: https://critmumbai.files.wordpress.com
[33] A. Aftab, Are the third world cities sustainable. Allied Publishers, 2005.
[34] G. H. Rosenfield and K. Fitzpatrick-Lins, "A coefficient of agreement as a measure of thematic classification accuracy.," Photogramm. Eng. Remote Sensing, vol. 52, no. 2, pp. 223–227, 1986.
[35] H. T. T. Nguyen, T. M. Doan, E. Tomppo, and R. E. McRoberts, "Land Use/Land Cover Mapping Using Multitemporal Sentinel-2 Imagery and Four Classification Methods—A Case Study from Dak Nong, Vietnam," Remote Sens., vol. 12, no. 9, p. 1367, 2020, doi: 10.3390/rs12091367.
[36] Z. Xie, Y. Chen, D. Lu, G. Li, and E. Chen, "Classification of Land Cover, Forest, and Tree Species Classes with ZiYuan-3 Multispectral and Stereo Data," Remote Sens., vol. 11, no. 2, p. 164, 2019, doi: 10.3390/rs11020164.
[37] L. N. Kantakumar and P. Neelamsetti, "Multi-temporal land use classification using hybrid approach," Egypt. J. Remote Sens. Sp. Sci., vol. 18, no. 2, pp. 289–295, 2015, doi: 10.1016/j.ejrs.2015.09.003.
[38] K. Islam, M. Jashimuddin, B. Nath, and T. K. Nath, "Land use classification and change detection by using multi-temporal remotely sensed imagery: The case of Chunati wildlife sanctuary, Bangladesh," Egypt. J. Remote Sens. Sp. Sci., vol. 21, no. 1, pp. 37–47, 2018, doi: 10.1016/j.ejrs.2016.12.005.
[39] A. Tariq and F. Mumtaz, "Modeling spatio-temporal assessment of land use land cover of Lahore and its impact on land surface temperature using multi-spectral remote sensing data," Environ. Sci. Pollut. Res., vol. 30, no. 9, pp. 23908–23924, 2022, doi: 10.1007/s11356-022-23928-3.
[40] J. Cohen, "Weighted kappa: Nominal scale agreement provision for scaled disagreement or partial credit.," Psychol. Bull., vol. 70, no. 4, p. 213, 1968.
[41] H. Xiao and Q. Weng, "The impact of land use and land cover changes on land surface temperature in a karst area of China," J. Environ. Manage., vol. 85, no. 1, pp. 245–257, 2007, doi: 10.1016/j.jenvman.2006.07.016.
[42] B.-C. Gao, "NDWI A Normalized Difference Water Index for Remote Sensing of Vegetation Liquid Water From Space," Remote Sens. Environ., vol. 58, no. 3, pp. 257–266, 1996, doi: 10.24059/olj.v23i3.1546.
[43] Y. Zha, J. Gao, and S. Ni, "Use of normalized difference built-up index in automatically mapping urban areas from TM imagery," Int. J. Remote Sens., vol. 24, no. 3, pp. 583–594, 2003, doi: 10.1080/01431160304987.
[44] S. A. Salman, S. Shahid, H. A. Afan, M. S. Shiru, N. Al-Ansari, and Z. M. Yaseen, "Changes in climatic water availability and crop water demand for Iraq region," Sustainability, vol. 12, no. 8, p. 3437, 2020.
[45] USGS, "Landsat Science Data User's handbooks," 2001. [Online].
Available: https://www.usgs.gov/land-resources/nli/landsat/landsat- 8-data-users-handbook
[46] J. C. Semenza et al., "Heat-Related Deaths during the July 1995 Heat Wave in Chicago," N. Engl. J. Med., vol. 335, no. 2, pp. 84–90, 1996, doi: 10.1056/nejm199607113350203.
[47] X. Chen and Y. Zhang, "Impacts of urban surface characteristics on spatiotemporal pattern of land surface temperature in Kunming of China," Sustain. Cities Soc., vol. 32, pp. 87–99, 2017, doi: 10.1016/j.scs.2017.03.013.
[48] A. Balew and T. Korme, "Monitoring land surface temperature in Bahir Dar city and its surrounding using Landsat images," Egypt. J. Remote Sens. Sp. Sci., vol. 23, no. 3, pp. 371–386, 2020, doi: 10.1016/j.ejrs.2020.02.001.
[49] N. K. Yadav, S. S. Mitra, A. Santra, and A. K. Samanta, "Understanding Responses of Atmospheric

Pollution and its Variability to Contradicting Nexus of Urbanization–Industrial Emission Control in Haldia, an Industrial City of West Bengal," J. Indian Soc. Remote Sens., vol. 51, no. 3, pp. 625–646, 2023, doi: 10.1007/s12524-022-01649-x.
[50] I. Hoque and S. K. Lepcha, "A geospatial analysis of land use dynamics and its impact on land surface temperature in Siliguri Jalpaiguri development region, West Bengal," Appl. Geomatics, vol. 12, no. 2, pp. 163–178, 2019, doi: 10.1007/s12518-019-00288-1.
[51] F. Zhang et al., "Dynamics of land surface temperature (LST) in response to land use and land cover (LULC) changes in the Weigan and Kuqa river oasis, Xinjiang, China," Arab. J. Geosci., vol. 9, no. 7, 2016, doi: 10.1007/s12517-016-2521-8.
[52] S. Hussain and S. Karuppannan, "Land use/land cover changes and their impact on land surface temperature using remote sensing technique in district Khanewal, Punjab Pakistan," Geol. Ecol. Landscapes, vol. 7, no. 1, pp. 46–58, 2021, doi: 10.1080/24749508.2021.1923272.
[53] S. Hussain et al., "Assessment of land use/land cover changes and its effect on land surface temperature using remote sensing techniques in Southern Punjab, Pakistan," Environ. Sci. Pollut. Res., vol. 30, no. 44, pp. 99202–99218, 2022, doi: 10.1007/s11356-022-21650-8.